INFLUENCE OF THE LINKER TYPE ON THE AU–S BINDING PROPERTIES OF THIOL AND DISULFIDE-MODIFIED DNA SELF-ASSEMBLY ON POLYCRYSTALLINE GOLD

Lidia Martínez,*[a] Laura G. Carrascosa,[bc] Yves Huttel,[a] Laura M. Lechuga[bc] and Elisa Román[a]

[a] *Instituto de Ciencia de Materiales de Madrid (ICMM-CSIC), Cantoblanco, 28049 Madrid, Spain. E-mail: lidia.martinez@icmm.csic.es; Fax: +(34)913720623; Tel: +(34)913349000*

[b] *Nanobiosensors and Molecular Nanobiophysics Group, CIBER of Bioingeneering, Biomaterials and Nanomedicine (CIBER-BBN). 08193 Bellaterra, Barcelona, Spain*

[c] *Nanobiosensors and Molecular Nanobiophysics Group, Research Center on Nanoscience and Nanotechnology (CIN2) CSIC-ICN. 08193 Bellaterra, Barcelona, Spain*

ABSTRACT

We investigate the Au–S binding properties of thiol and disulfide-modified DNA on polycrystalline gold by means of X-ray photoelectron spectroscopy in conditions close to dynamic processes of biosensors. The dependence of the immobilisation period on the quality and density of the self-assembly process of thiol ($SH–(CH_2)_6–DNA$), disulfide ($DNA–CH_2)_6–SS–(CH_2)_6–DNA$ and $DMTO–SS–(CH_2)_6–DNA$) sulfur-modified oligonucleotide solutions (1 mM) that are employed for bioreceptor immobilisation is analysed. Two electronic components are found in the analysis of the S 2p core levels. One of them is clearly associated to thiolate formation, while the other can be associated to different origins. In order to identify the origin of this last component, a quantification of the non-specifically adsorbed species has been performed by rinsing the self-assembled monolayers (SAMs) with a mercapto hexanol (MCH) solution. It has been found that non-specifically adsorbed species contribute only partially to the appearance of this sulfur peak component in SAMs formed from disulfides. Electron bombardment was performed to study the evolution of this component as a consequence of surface degradation due to radiation effects. The results are also correlated with the possible presence of disulfides. We found that MCH is not stable during the measurements. The evolution of this compound and the possible causes for this behaviour are discussed.

INTRODUCTION

Self-assembled monolayers (SAMs) are organic assemblies formed by the adsorption of molecular constituents from liquid or gas phases onto solid surfaces where the adsorbates organize spontaneously into semicrystalline assemblies.[1,2] They have attracted considerable interest due to their ability to control surface properties in a variety of technologies such as wetting, adhesion, lubrication, corrosion, and sensing on surfaces and interfaces in many applications.[2–4] Among different kinds of SAMs, films formed from thiol-derived molecules probably offer the best available combination of high structural order, flexibility in the end groups exposed at the extreme surface, and simplicity in the preparation.[2,3,5,6] Previous research has demonstrated that high-quality SAMs can be also formed from disulfides, as S–S bond cleavage takes place during adsorption. However, they tend to precipitate into multilayers if sample preparation conditions are not carefully controlled[1] and the assembly process is slower than that observed with thiols, which results in different properties than those of thiol-derived SAMs.[2]

The knowledge about the molecule adsorption structure is determinant for the understanding of the interaction aspects between the substrate and the molecule.[7] This self-assembly mechanism has a strong impact on the utility of the surface for practical purposes in lubrication, catalysis, adhesion and sensor devices. In particular, thiols chemisorbed on metallic surfaces form thin films that are suitable for application as electrochemical sensors.[9] These sensors are promising in anchoring large sulfur-modified

biomolecules such as DNA to gold surfaces. Up to now, most articles concerning thiol-SAM deals with simpler systems, such as alkanethiols. However, in the last few years there has been a growing interest in thiol-ended DNA strands, where additional interactions between strands must be taken into account. Methods for surface-immobilizing single-strand nucleic acids that preserve their original hybridization specificity with minimized nonspecific interactions remain an important issue for improving the performance of DNA microarray and biosensor applications,[10,11] that can also be used for genomics applications or protein detection as well as immobilize plasmid DNA for subsequent delivery to cells.[11]

In this work, we compare the self-assembly process of thiol and disulfide sulfur-modified oligonucleotides on polycrystalline gold surfaces. It is worth mentioning that polycrystalline surfaces were chosen as substrates because they are closer to real cases than single crystal surfaces and, therefore, they are the most adequate substrates for the study of real processes for biosensor applications. The formation of SAMs kinetically proceeds through two phases: the first one, where adsorption of molecules on the substrate takes place during the first few minutes, and the second and longer step where organization of the molecules occurs.[5,12] In this work, we have chosen an immobilization time of 5 min in order to simulate dynamic processes for sensor applications, which also can be correlated to the first step of SAM formation. A longer immobilisation time was also tested for correlation purposes with the second phase for SAM formation. For the analysis of the systems, there are several surface characterisation techniques that have been used to study the properties and structures of self-assembled monolayers on Au surfaces. Duwez[5] and Vericat *et al.*[6] presented in their respective reviews a summary of all these techniques. Among them, XPS is one of the most widely used techniques for the characterization of organic– inorganic interfaces.[13] It has been used to investigate the structure and organization of thiols or disulfides on gold and, in particular, to characterize the S–Au bond.[14,15] In this study we will focus on the characteristics of the sulfur bond with gold to evaluate the efficiencies to chemisorb during self-assembly depending on the linker. We present our results on the identification and quantification of the chemisorbed species for two immobilisation times and discuss other contributions such as physisorbed or disulfide species in the systems under study as well as radiation damage effects. An effort has been performed to study the immobilisation process in systems as close as possible to real biosensors, *i.e.* nano- mechanical and surface plasmon resonance biosensors, by the adequate choice of substrate, immobilisation times and rinsing procedures.

MATERIAL AND METHODS

Sample preparation

Gold coated surfaces prepared by thermal evaporation of 2 nm of chromium and 45 nm of gold onto clean glass slides were used as substrates. Single stranded DNA oligonucleotides 12 mer (monomeric unit) long (5'-AACGACGGCCAG-3') HPLC-purified were purchased from Genomechanix, LLC (USA) bearing at the 5' end a thiol modification as follows: the thiol *SH*–$(CH_2)_6$–*DNA* (hereafter called DNA–SH); the symmetric disulfide form *DNA*–$(CH_2)_6$–*SS*–$(CH_2)_6$–*DNA* (hereafter called DNA–SS–DNA) and *DMTO*–*SS*–$(CH_2)_6$–*DNA* (hereafter called DNA–SS–DMTO), an asymmetric disulfide form in which the disulfide group bridges the DNA molecule with a small uncharged molecule, dimetoxitrityl group (DMTO). After deposition of the gold on the glass substrates, the samples were extracted from the ultra high vacuum deposition chamber and immobilization procedures were performed immediately with a 1 mM concentration of the oligo sample prepared in a buffered solution (50 mM Sodium Phosphate— 1 M NaCl). DNA solution was gently dropped on the gold surface, and left for 5 min and 15 h. After these immobilization periods, the samples were rinsed with deionised water and dried under nitrogen flux. The shorter immobilisation time was chosen in order to reproduce the dynamical case of the biosensor preparation and the longer immobilisation time was chosen

to study the longer-term behaviour. Post-treatment with mercaptohexanol (MCH) was also performed on a series of DNA monolayers previously immobilised. The treatment was carried out immediately after DNA immobilization by gently dropping a 1 mM solution of MCH in buffered solution (50 mM Sodium Phosphate—1 M NaCl) for 5 min. Then, samples were rinsed with deionised water and air dried under nitrogen flux. References samples with only MCH were also prepared.

X-ray photoelectron spectroscopy (XPS)

The XPS measurements were performed in an ultra high- vacuum (UHV) chamber with a base pressure of 1×10^{-10} mbar. The angle between the hemispherical analyzer (Specs-PHOIBOS100) and the plane of the surface was kept at 601 and the X-ray radiation was the Mg-Ka line (1253.6 eV). The survey spectra were recorded with a photon energy step of 0.25 eV and a pass energy of 40 eV, and the S 2p and Au 4f core levels with a photon energy step of 0.1 eV and a pass energy of 15 eV. In order to increase the signal-to-noise ratio at the S 2p core level spectra, a number of scans were accumulated for each sample. The analysis of the individual scans (acquired in groups of 150 accumulated scans) was performed in order to ensure the stability of each system in UHV. Prior to the data analysis, the contributions of the Mg-Ka satellite lines were subtracted and the spectra were subjected to linear background subtraction formalism. The binding energy (BE) scale was calibrated with respect to the Au $4f_{7/2}$ peak at 83.8 eV. Fittings were carried out using Gaussian–Lorentzian doublets (GL) with the standard spin–orbit splitting of 1.2 eV, a S $2p_{1/2}$/S $2p_{3/2}$ branching ratio of 1 : 2[16–18] and the same Full Width at Half Maximum (FWHM) (1.3 0.1 eV). This value is close to 1.03 eV as reported by Wackerbarth *et al.*[16] The reason for the wider FWHM in our case could be due to the different preparation method of the polycrystalline gold substrate. Using the equation:

$$I_d = I_{Au} [1 - \exp(-d/l \sin y)] \qquad (1)$$

we have estimated the photoemission intensity from the outermost gold layer (I_d), where d is the thickness of this outermost layer (3 Å) (see inset of Fig. 1), I_{Au} is the photo- emission intensity from the whole gold substrate, l is the inelastic mean free path (22 Å) and y is the take-off angle between the sample and the analyser (601).

With this calculation of I_d and considering the whole photoemission intensity from the sulfur, I_s, we have calculated the I_s/I_d ratio in a way that we are more sensitive to changes in the S coverage of each system. With this ratio, it is possible to extrapolate the S surface density in terms of molecules cm^{-2}. It must be taken into account that these values are obtained after a series of approximations and will be mainly used to compare the different systems studied in this work. The attenuation due to the organic layer has not been taken into account in order to avoid the inclusion of additional variables in this approximation, as is expected to be similar for electrons coming from both the Au and S atoms. It should be noted that the attenuation due to the organic layer would probably slightly increase the I_s/I_d ratios.

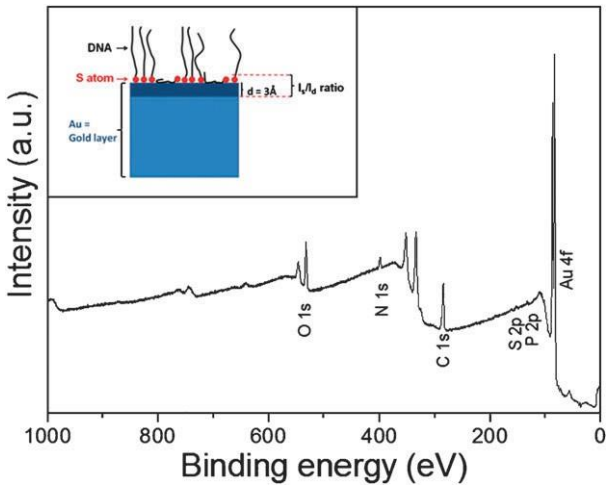

Fig. 1 XPS survey scan of one of the samples. The inset represents a scheme of the approximation used for the calculation of the Au signal corresponding to the top surface layer that is used for the S/Au ratio estimation.

Electron bombardment

A series of samples were irradiated with electrons of 2 keV kinetic energy. The electron dose calculated by the product of the current density and the exposure time:

$$D\ [\mathrm{C/cm^2}] = J\ [\mathrm{A/cm^2}]\ t\ [\mathrm{s}] \qquad (2)$$

was approximately 9×10^{-4} C cm^{-2}. According to Pantano and Madey,[19] the damage threshold (D_d) or minimum electron dose required for damage to be detectable can be defined for electron-stimulated change in the surface concentration, DN. The concentration of undamaged species at any time, $N(t)$, obeys a first order relation:

$$N(t) = N_0 \exp\left(-\frac{I_\varepsilon Q}{A\varepsilon} \cdot t\right) \qquad (3)$$

where N_0 is the initial undamaged concentration (molecules cm^{-2}) within the analysis region, I_e is the total beam current, A is the irradiated area, e is the electronic charge 1.6×10^{-19} C and Q is the effective cross-section (cm^2) for electron stimulated decrease in the ratio $N(t)/N_0$. If we assume that a 10% change in concentration of a given species can be detected, D_d can be calculated assuming that detectable damage occurred when D$N/N = 0.1$. Thus, from eqn (2) and (3), the electron dose required to cause detectable damage is:

$$D_d = J{\cdot}t = Ie/A{\cdot}t \sim 0.11 \in /Q \qquad (4)$$

Since the typical cross-section for stable systems is 10^{-17} cm^2, $D_d \approx 1.7 \times 10^{-4}$ C cm^{-2}. The typical electron doses employed in this study were 9×10^{-4} C cm^{-2}, which is in the range to generate damage to the SAMs.

RESULTS AND DISCUSSION

From the survey scans (Fig. 1), only species coming from the studied systems were detected and no other elemental signals were observed. The dependence of the sulfur bond characteristics upon different

parameters is studied by the analysis of the S 2p core level.

Dependence on the immobilisation period

Fig. 2 displays the analysis of the S 2p core levels for short (5 min) and long (15 h) immobilisation periods. In all cases, two doublets were used for the fitting procedure. The first doublet, labelled S1, was found at a binding energy of the $2p_{3/2}$ peak at 161.9 0.5 eV, while the second doublet (S2) was located at a binding energy of the $2p_{3/2}$ peak at 163.4 0.5 eV. According to the literature, the S1 component corresponds to S bound to gold in form of thiolate.[20–29] Thiols can chemisorb through the sulfur bond due to the sulfur affinity for gold.[30] Disulfides (from DNA–SS–DNA and DNA–SS–DMTO) can also partially adsorb in form of thiolates by dissociative adsorption of the disulfide bridge, which results in an increased stability and is more likely to occur than molecular adsorption.[20,21,31–33] The interpretation of the S2 contribution is less straightforward. There are several explanations in the literature for the S 2p peaks in the energy range between 163 and 164 eV. Most of them are associated to physisorbed species,[16,22,34] to the presence of the disulfide specie[21,23–25] or to the formation of sulfur species due to damage from ionising radiation.[22,26]

Our results confirmed that an immobilisation of 5 min (Fig. 2a–c) leads to an important chemisorption of modified DNA, where the thiolate formation (S1) is predominant for the three solutions employed. The DNA–SH and DNA–SS–DNA solutions presented a higher efficiency for this thiolate formation, while it is significantly reduced in the case of DNA–SS–DMTO solution. The sulfur surface densities (included in each graph) calculated for the DNA–SS–DMTO and DNA–SS–DNA samples are in the range of those reported by other authors,[35-36] although in the case of DNA–SH, the 9.9 x 10^{13} molecules cm^{-2} value is higher than those reported (1–6 x 10^{13} molecules cm^{-2}). Commercial thiol modified strands (DNA–SH) can contain an excess of sulfur as a consequence of contamination.37 These sulfur contaminants are usually oxidised, but in our case, no evidence of oxidized sulfur was found in any of the samples. Furthermore, increasing amounts of nitrogen and phosphorous were detected with longer immobilization times, which confirmed that the sulfur signal comes from the modified DNA. Hence, the surface densities calculated from our method could lead to higher values than those reported in the literature. Nevertheless, by comparing the three solutions employed it can be concluded that the thiol linker leads to a denser packing than disulfides after short immobilisation periods.

Fig. 2d–f displays the S 2p core level spectra of the samples after an immobilisation period of 15 h. Longer immobilisation periods are expected to facilitate the reorganization of the films formed at shorter periods and, therefore, to increase the thiolate contribution (S1). However, only DNA–SS–DMTO presented an increase in this thiolate contribution in comparison to 5 min immobilisation. DNA–SS–DNA presented the opposite trend. Longer immobilisation periods resulted in a reduction of the proportion of the thiolate contribution. In this case, a lower S coverage was also detected. This reduction of the S coverage can be attributed to thiolate desorption to the aqueous phase *via* disulfide formation during long immobilisation periods.[38] In addition, the higher steric hindrance of this molecule is likely to make more difficult the approach to the surface of new molecules. In the case of DNA–SH, a similar proportion of thiolates was observed compared to shorter immobilisation periods. This system it is the only one that presented a clear increment in the S coverage. This evolution is likely to indicate that the SAMs formation from thiols is highly favoured in comparison to disulfides.

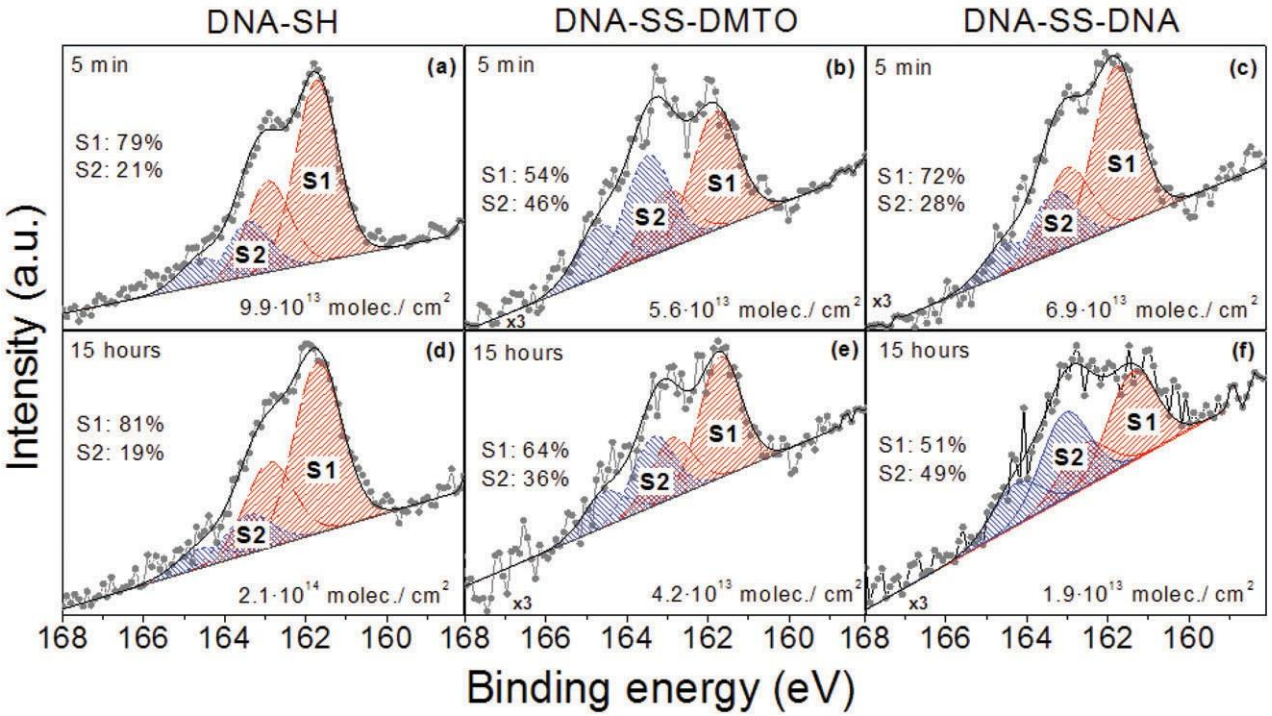

Fig. 2 S 2p core levels of DNA–SH, DNA–SS–DMTO and DNA–SS–DNA for immobilizations of 5 min (a–c) and 15 h (d–f). —●— experimental points —— fit. Additional information about the proportion of the components and surface density in terms of molecules per square centimetre is also included.

Studies performed by other authors[16,21,33,39,40] were not able to distinguish between SAMs formed from alkane-thiols or disulfides, as both precursors form the same species on the surfaces. In the case of DNA strands SAMs, we found differences between SAMs formed from thiols or disulfides. The results evidenced that DNA–SH is more effective in the formation of a dense and properly bonded SAM than both disulfide-modified DNA studied here. Furthermore, it is important to point out the short time needed to obtain a significant proportion of chemisorbed species from DNA–SH for the biosensor applications.

In order to fully understand the SAM formation from these modified DNA, it is necessary to evaluate the factors that contribute to the S2 component. In the following sections we present a study of the origin of this contribution in our particular system.

Desorption of non-specifically adsorbed molecules with MCH

With the aim of estimating the amount of physisorbed species that contribute to the S2 component, a treatment was carried out with MCH. It is well established that this compound controls the film formation process as well as the conformation of the surface-anchored DNA oligonucleotides.[41] It prevents the non-specific adsorption of modified DNA to the surface by removing the physisorbed species from the surface and increasing the specific attachment of thiolated groups.[10] The MCH treatment was carried out on samples with 5 min immobilization (equivalent to the ones presented in Fig. 2a–c). The corresponding XPS spectra are displayed in Fig. 3a–c. After the MCH treatment, the S coverage significantly increases in all cases. This increment is less significant in the DNA–SH sample as a result of the smaller number of unoccupied sites on the Au surface that are available for chemisorption after the efficient immobilization of the DNA–SH solution. For that case, the proportion of the S 2p core level components remained almost unchanged with variations close to the experimental uncertainty. Both facts

are an indication of the high efficiency of the thiol linker type, where no contribution to the S2 component can be attributed to physisorbed species. On the other hand, the MCH treatment was effective in the removal of the physisorbed species from DNA–SS–DMTO and DNA–SS–DNA cases, possibly due to the different nature of the SAM formed from these solutions. DNA–SS–DMTO samples presented the highest proportion of physisorbed species at short immobilization periods (Fig. 2b) and the MCH treatment induced a reduction of the S2 component (Fig. 3b). From this decrease it can be concluded that the 21% of the sulfur present on the original sample was in the form of physisorbed species. In the case of DNA–SS–DNA this amount represents only 8%. Even if the efficiency of MCH to chemisorb on the gold surface is known to be very high, the possibility of physisorption cannot be completely ruled out. However, we can assume that the efficiency of MCH to remove physisorbed species is the same independently of the DNA solution and, therefore, the different response to the MCH treatment observed in the case of the DNA–SH samples is consistent. The kinetics of the thiolate formation is faster from thiol than from disulfides. Therefore, after 5 min most part of the sulfur is already chemisorbed in the DNA–SH case and no physisorbed species were detected. Consequently, this linker is particularly suitable for biosensor applications.

From the analysis of the MCH treatment it can be concluded that the S2 component in the S 2p core level spectra can be partially correlated with the presence of physisorbed species, but other species do also contribute to the S2 component.

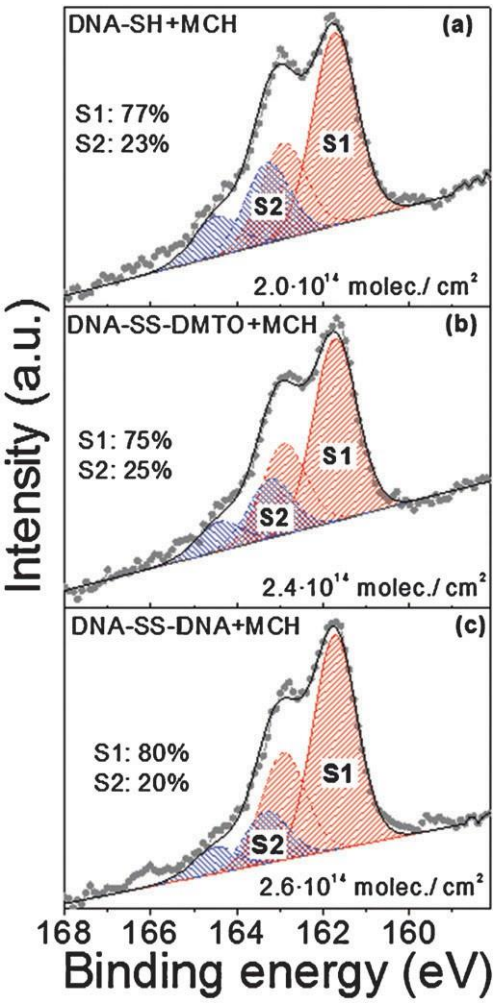

Fig. 3 S 2p core levels of (a) DNA–SH, (b) DNA–SS–DMTO and (c) DNA–SS–DNA treated with MCH immediately after their prepara- tion. —●— experimental points —— fit.

Dependence of surface degradation upon electron bombardment

Since it has been reported in the literature that damage from ionising radiation can be the origin of the S2 component, we have performed additional experiments in order to evaluate this effect in our particular systems. As radiation-induced damages are due to the primary and secondary electron emissions,[6,14] electron bombardment was performed on two of the systems previously analysed using the conditions described in the experimental section.

In Fig. 4a–c the XPS spectra of the SAMs immobilised for 15 h (from Fig. 2d–f) after electron irradiation are displayed. A clear increase in the S2 component (B10%) was only observed in the case of DNA–SH sample. The other samples presented a much lower S coverage and, thus, the variation in the S2 component as well as the S coverage after electron bombardment is within the experimental uncertainty. The effects of radiation-induced damage described in the literature are related to the formation of new species such as disulfides.[14] In the case of alkanethiols it has been reported that the radiation-induced damage could be related to an incorporation of sulfur into the alkyl matrix through its bonding to a carbon radical in the adjacent aliphatic chains,[42] while in the case of DNA strands, ionizing radiation induces DNA strand breaks.[43] In our case, the modifications observed in the analysis of the S 2p core level spectra lay in the binding energy range of S2 that corresponds to disulfides.[21,23–25] From the variations observed in this component after electron bombardment, it can be concluded that the initial concentration

of species contributing to the S2 component is more important than the increase in this component after electron bombardment and, therefore, this component cannot be attributed exclusively to radiation-induced damage.

A second study of the effect of electron bombardment on SAM degradation has been performed on samples rinsed with MCH (from Fig. 3a–c). The removal of non-specifically adsorbed species from the surface would make the identification of the XPS components associated to radiation-induced damage more straightforward. Fig. 4d–f displays the XPS spectra of these samples. Electron bombardment induced an increase in the proportion of the S2 component in all the samples (between 17% and 23%), although at the same time, a reduction in the S coverage was observed. Other authors[44–46] previously reported a small loss of material upon irradiation time, where the main effect is a decrease in the thiolate contribution. In our case we also observed a clear reduction of the thiolate contribution. The breaking of the thiolate bond is reported to induce the formation of disulfide species.[14,18] By comparing the proportion of the S2 component before and after electron bombardment relative to the S coverage, we could deduce that the S2 component contribution represents no more than a 2.5% of the formation of disulfides in the DNA–SH sample. On the other samples, the differences were found to be smaller and, therefore, the results were not conclusive. However, the present results clearly show that the S coverage reduction is mainly due to the thiolate desorption.

Degradation of MCH

Since a series of samples were treated with MCH, we have measured the evolution of a reference MCH sample upon the number of XPS scans in order to separate the contribution of the MCH from the other adsorbed molecules in the S 2p core level spectra. This sample also presented two contributions to the S 2p core level spectra. However, in that particular case, we observed a simultaneous reduction of the S1 component intensity and S coverage upon the number of XPS scans or X-ray irradiation time, similar to those observed after electron bombardment of samples rinsed with MCH in Fig. 4d–f, which was attributed to thiolate desorption. Fig. 5 represents the evolution of the S1 and S2 components relative to the S coverage upon the X-ray exposure. The S1 component presented an exponential decay according to: $y = 1 + 16\exp(-x/1570)$, indicative of thiolate removal from the surface. The S2 component presented a smoother linear decrease according to: $y = 11.81 - 0.002\,x$ with the number of scans. In this case, no disulfide formation could be confirmed, as the S2 component also diminished. The insets in Fig. 5 represent the S 2p core levels corresponding to initial, medium and final scans of the experiments, where it can be easily observed the evolution of the proportion of the sulfur components. In conclusion, MCH suffered degradation with increasing number of XPS scans or X-ray irradiation time. The S coverage decreased with the increasing number of scans mainly due to thiolate desorption (S1 component) from the Au surface. With this result it can also be concluded that the evolution observed after electron bombardment of the samples treated with MCH (Fig. 4d–f) are consequence of the MCH itself, which seemed to be more sensitive to radiation damage than the DNA strands. These results are in contradiction with the findings of Kummer *et al.*[41], which reported X-ray radiation induced damage of the MCH SAMs with very limited effect on the sulfur atoms bounded to the gold surface, even for long-term irradiation (referred to 75 min). The discrepancy might be due to the differences in the sample preparation (substrate preparation, immobilisation times and rinsing procedures, *etc.*), which in turn affect the SAMS's quality (density of molecules, bond types, *etc.*) and is likely to modify the SAMs' response under X-ray irradiation. This clearly illustrates the need to study systems as close as possible to the real cases in order to understand the phenomena in real sensors as we have tried to perform here.

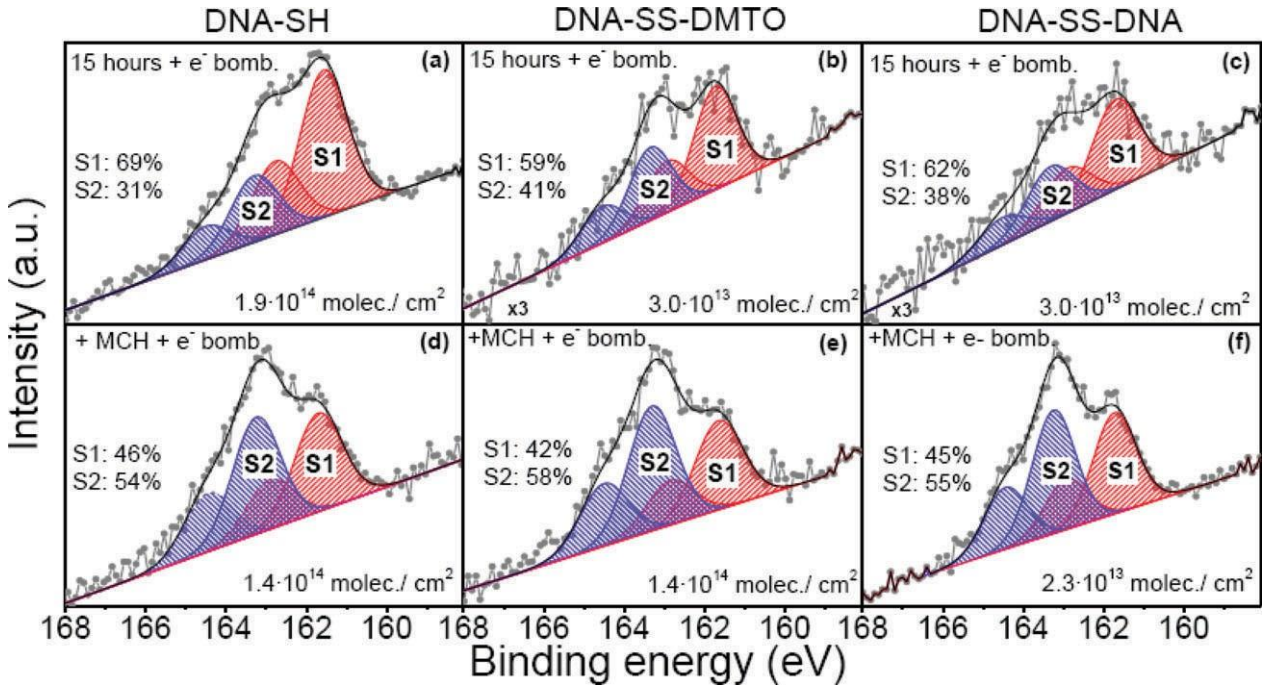

Fig. 4 S 2p core levels of DNA–SH, DNA–SS–DMTO and DNA–SS–DNA after electron bombardment of the samples immobilised for 15 h (a–c) and the samples rinsed with MCH immediately after their preparation (d–f). The electron dose was 0.9 mC cm^{-2}. —●— experimental points —— fit.

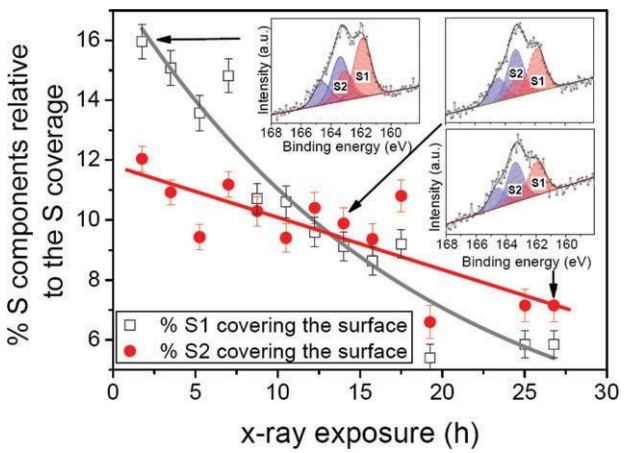

Fig. 5 Evolution of the S 2p core level components of the MCH reference sample relative to the sulfur coverage upon the X-ray exposure. The insets are S 2p core levels of the MCH sample at the beginning, middle and end of the experiment.

Conclusions

We presented a XPS study of the sulfur–gold bond of DNA- modified oligonucleotides, where the experimental conditions were chosen in order to be as close as possible to the real case of biosensors. The results obtained in this work evidenced that short immersion periods of 5 min are long enough to obtain a dense S coverage over the polycrystalline gold with the three solutions employed, where most of the sulfur present is covalently bonded to Au in the form of thiolate (S1). Longer immersion periods lead to an enhancement of the S coverage with the DNA–SH solution. Apart from thiolate formation, there are other contributions to the S 2p core level with proportions that directly depend on the linker type. The origin of these other contributions are physisorbed species, radiation- induced damage (in a limited proportion) and, in agreement with previous studies reported in the literature, disulfide species.

The linker employed is crucial on the final characteristics of the SAMs formed. Thiol-modified oligonucleotide (DNA–SH) is clearly more effective than disulfides and, therefore, is the most suitable for biosensor applications. With this linker we obtained a denser S coverage with a higher proportion of chemisorbed species in form of thiolate (around 80%). According to our results, no significant contribution of physisorbed species were found with this linker and only a small proportion of the sulfur signal could be related to radiation-induced damage (less than 3%). Consequently, the remaining sulfur should be in the form of disulfide species, as a result of the recombination of the nearest-neighbour thiolates on the surface of monolayers formed from thiols and disulfides.[47]

The efficiency of the DNA–SS–DMTO solution in the S–Au bond formation is lower than DNA–SH solution. Even though longer immersion times lead to an increase in the S coverage, the proportion of chemisorbed species is still comparatively lower for DNA–SS–DMTO. This result is in accordance to the slower kinetic for chemisorption of disulfide species in comparison to thiols. With this linker, the amount of physisorbed species represents about 21% of the sulfur, which is the highest proportion found for the three sulfur-modified oligonucleotide solutions. In addition, the lower coverage obtained with this linker reflected that molecular adsorption can occur as a consequence of the low steric impediment of the DMTO molecule that could enable the simultaneous creation of the two chemisorption sites required for molecular adsorption.[40] This kind of adsorption could explain the higher percentage of the S2 component obtained with this linker.

Finally, the DNA–SS–DNA linker induced a similar proportion of thiolates on the gold surface than DNA–SH at short immobilisation times although with a lower coverage. The larger size of DNA chain in comparison to the DMTO enhances the S–S cleavage at the beginning of the assembly process, resulting in a higher percentage of thiolate formation. However, longer immobilisation periods lead to a decrease in the S coverage and in the proportion of thiolates. Therefore, even though the S coverage as well as the proportion of thiolates obtained with DNA–SS–DNA are similar to DNA–SH at low immobilization times, the evolution of both systems after 15 h indicate that the nature of the SAM formed in each case is different.

MCH is sensitive to radiation damage as can be inferred from the decrease in the S coverage as a consequence of thiolate desorption.

Acknowledgements

L. M., Y. H. and E. R. acknowledge the Nanoselect project (CSD2007-00041) from the Spanish Ministry for Innovation and Science. Prof. C. Ocal is greatly acknowledged for critical reading of the manuscript.

REFERENCES

1 J. C. Love, L. A. Estroff, J. K. Kriebel, R. G. Nuzzo and G. M. Whitesides, *Chem. Rev.*, 2005, 105, 1103–1169.

2 M. I. Bełthencourt, L. Srisombat, P. Chinwangso and T. Randall Lee, *Langmuir*, 2009, 25, 1265–1271.

3 M. Zharnikov and M. Grunze, *J. Phys.: Condens. Matter*, 2001, 13, 11333–11365.
4 P. Fenter, A. Eberhardt and P. Eisenberg, *Science*, 1994, 266, 1216–1218.
5 A. S. Duwez, *J. Electron Spectrosc. Relat. Phenom.*, 2004, 134, 97–138.
6 C. Vericat, M. E. Vela, G. A. Benitez, J. A. Martin Gago, X. Torrelles and R. C. Salvarezza, *J. Phys.: Condens. Matter*, 2006, 18, R867–R900.
7 S. Yagi, Y. Nakano, E. Ikenaga, S. A. Sardar, J. A. Syed, K. Tanaka, E. Hashimoto and M. Taniguchi, *Surf. Sci.*, 2004, 566–568, 746–750.
8 A. J. Leavitt and T. P. Beebe, Jr., *Surf. Sci.*, 1994, 314, 23–33.
9 J. A. Syed, S. A. Sardar, S. Yagi and K. Tanaka, *Thin Solid Films*, 2006, 515, 2130–2136.
10 C.-Y. Lee, P. Gong, G. M. Harbers, D. W. Grainger, D. G. Castner and L. J. Gamble, *Anal. Chem.*, 2006, 78, 3326–3334.
11 S. Choi and W. L. Murphy, *Langmuir*, 2008, 24, 6873–6880.
12 G. Hahner, C. Woll, M. Buck and M. Grunze, *Langmuir*, 1993, 9, 1955–1958.
13 J. A. Syed, S. A. Sardar, S. Yagi and K. Tanaka, *Surf. Sci.*, 2004, 566–568, 597–602.
14 T. Ishida, M. Hara, I. Kojima, S. Tsuneda, N. Nishida, H. Sasabe and W. Knoll, *Langmuir*, 1998, 14, 2092–2096.
15 P. Feulner, T. Niedermayer, K. Eberle, R. Schneider, D. Menzel, A.Baumer, E. Schmich, A. Shaporenko, Y. Tai and M. Zharnikov, *Surf. Sci.*, 2005, 593, 252–255.
16 H. Wackerbarth, R. Marie, M. Grubb, J. Zhang, A. G. Hansen, Ib. Chorkendorff, C. B. V. Christensen, A. Boisen and J. Ulstrup, *J. Solid State Electrochem.*, 2004, 8, 474–481.
17 M. C. Bourg, A. Badia and R. B. Lennox, *J. Phys. Chem. B*, 2000, 104, 6562–6567.
18 D. G. Castner, K. Hinds and D. W. Grainger, *Langmuir*, 1996, 12, 5083–5086.
19 C. G. Pantano and T. E. Madey, *Appl. Surf. Sci.*, 1981, 7, 115–141.
20 H.-M. Huang, C.-Y. Chang, I.-C. Liu, H.-C. Tsai, M.-K. Lai and R. C.-C. Tsiang, *J. Polym. Sci., Part A: Polym. Chem.*, 2005, 43, 4710–4720.
21 C. D. Bain, H. A. Biebuyck and G. M. Whitesides, *Langmuir*, 1989, 5, 723–727.
22 O. Cavalleri, L. Oliveri, A. Dacca` , R. Parodi and R. Rolandi, *Appl. Surf. Sci.*, 2001, 175–176, 357–362.
23 O. Cavalleri, G. Gonella, S. Terreni, M. Vignolo, P. Pelori, L. Floreano, A. Morgante, M. Canepa and R. Rolandi, *J. Phys.: Condens. Matter*, 2004, 16, S2477–S2482.
24 M. Wirde, U. Gelius, T. Dunbar and D. L. Allara, *Nucl. Instrum. Methods Phys. Res., Sect. B*, 1997, 131, 245–251.
25 D. Zerulla, I. Uhlig, R. Szargan and T. Chasse, *Surf. Sci.*, 1998, 402–404, 604–608.
26 T. M. Willey, A. L. Vance, T. van Buuren, C. Bostedt, L. J. Terminello and C. S. Fadley, *Surf. Sci.*, 2005, 576, 188–196.
27 J. C. Munro and C. W. Frank, *Polymer*, 2003, 44, 6335–6344.
28 H.-L. Zhang, S. D. Evans, K. Critchley, H. Fukushima, T. Tamaki, F. Fournier, W. Zheng, S. Carrez, H. Dubost and B. Bourguignon, *J. Chem. Phys.*, 2005, 122, 224707.
29 E. O. Sako, H. Kondoh, I. Nakai, A. Nambu, T. Nakamura and T. Ohta, *Chem. Phys. Lett.*, 2005, 413, 267–271.
30 D. J. Lavrich, S. M. Wetterer, S. L. Bernasek and G. Scoles, *J. Phys. Chem. B*, 1998, 102, 3456–3465.
31 M. C. Vargas, P. Giannozzi, A. Selloni and G. Scoles, *J. Phys. Chem. B*, 2001, 105, 9509–9513.
32 R. Di Felice and A. Selloni, *J. Chem. Phys.*, 2004, 120, 4906–4914.
33 J. Noh and M. Hara, *RIKEN Rev.*, 2001, 54–57.
34 N. Garg, J. M. Friedman and T. R. Lee, *Langmuir*, 2000, 16, 4266–4271.
35 D. Y. Petrovykh, H. Kimura-Suda, Ll. J. Whitman and M. J. Tarlov, *J. Am. Chem. Soc.*, 2003, 125, 5219–5226.

36 A. B. Steel, R. L. Levicky, T. M. Herne and M. J. Tarlov, *Biophys. J.*, 2000, 79, 975–981.
37 C.-Y. Lee, E. Canavan, L. J. Gamble and D. G. Castner, *Langmuir*, 2005, 21, 5134–5141.
38 J. B. Schlenoff, M. Li and H. Ly, *J. Am. Chem. Soc.*, 1995, 117, 12528–12536.
39 H. A. Biebuyck, C. D. Bain and G. M. Whitesides, *Langmuir*, 1994, 10, 1825–1831.
40 C. Jung, O. Dannenberger, Y. Xu, M. Buck and M. Grunze, *Langmuir*, 1998, 14, 1103–1107.
41 K. Kummer, D. V. Vyalikh, G. Gavrila, A. Kade, M. Weigel-Jech, M. Mertig and S. L. Molodtsov, *J. Electron Spectrosc. Relat. Phenom.*, 2008, 163, 59–64.
42 M. Zharnikov, W. Geyer, A. Go̅lzha̅user, S. Frey and M. Grunze, *Phys. Chem. Chem. Phys.*, 1999, 1, 3163–3171.
43 Z. Cai, P. Cloutier, D. Hunting and L. Sanche, *J. Phys. Chem. B*, 2005, 109, 4796–4800.
44 D. Zerulla and T. Chasse̅, *Langmuir*, 1999, 15, 5285–5294.
45 M. Zharnikov, S. Frey, K. Heister and M. Grunze, *Langmuir*, 2000, 16, 2697–2705.
46 S. Frey, K. Heister, M. Zharnikov and M. Grunze, *Phys. Chem. Chem. Phys.*, 2000, 2, 1979–1987.
47 J. L. Trevor, K. R. Lykke, M. J. Pellin and L. Hanley, *Langmuir*, 1998, 14, 1664–1673.